*Circ J* 2005; **69:** 1052–1056

# Central Sympathetic Inhibition Augments Sleep-Related Ultradian Rhythm of Parasympathetic Tone in Patients With Chronic Heart Failure

Tsugiyoshi Yamazaki, MD; Hidetsugu Asanoi, MD; Hiroshi Ueno, MD; Kunihiro Yamada, MD; Junya Takagawa, MD; Tomoki Kameyama, MD; Tadakazu Hirai, MD; Shinji Ishizaka, MD; Takashi Nozawa, MD; Hiroshi Inoue, MD

**Background** Abnormal sleep dynamics in patients with heart failure is one of the mechanisms for the relative predominance of central sympathetic outflow over parasympathetic tone. This study was designed to examine whether central sympathoinhibition could improve the sympathovagal imbalance related to rapid-eye-movement (REM)/non-REM ultradian sleep rhythm in these patients.

**Methods and Results** Beat-by-beat RR intervals of overnight electrocardiogram were serially subject to power spectral analysis in 14 patients with chronic heart failure and 13 age-matched subjects with normal cardiac function. To assess autonomic sleep dynamics, the ultradian rhythm was extracted from all-night consecutive high-frequency (HF) components of heart rate variability (HRV) before and after administration of an $\alpha$2-adrenergic agonist, guanfacine. Night-time HRV in heart failure was characterized by an attenuated ultradian rhythm of HF-components with a concomitant reduction in averaged HF power. Guanfacine reduced blood pressure, heart rate, and plasma norepinephrine concentrations by 7%, 8%, and 34% ($p<0.01$), respectively. After guanfacine, HF power rose by 154% ($p<0.01$) with a prominent augmentation of the all-night ultradian rhythm (+361%, $p<0.01$).

**Conclusions** Central sympathoinhibition augments a sleep-related ultradian rhythm of parasympathetic tone, suggesting a potential benefit to autonomic balancing and sleep quality in patients with chronic heart failure. (*Circ J* 2005; **69:** 1052–1056)

**Key Words:** $\alpha$2-Adrenergic agonist; Heart rate variability; Power spectral analysis; Sympathovagal imbalance

Because enhanced sympathetic tone is major cause of progression of heart failure, a therapeutic target has been management of the sympathetic nerve activity in patients with chronic heart failure[1,2] Recently, sleep disturbance has received special attention in the pathogenesis of autonomic imbalance, which is potentially carried over from night into daytime[3,4] The autonomic function fluctuates depending on sleep dynamics when non-rapid-eye movement (REM) sleep is accompanied by an augmentation of parasympathetic tone and a depression of central sympathetic activity. In contrast, REM sleep is characterized by an augmentation of peripheral sympathetic tone, as confirmed by a microneurographic technique[5,6] Several previous studies have documented a lack of nocturnal reduction in heart rate (HR) in patients with heart failure as a consequence of hemodynamic abnormalities or sleep-disordered breathing[7–9] Therefore, one of the mechanisms for sympathoexcitation in heart failure could involve relative predominance of central sympathetic outflow over parasympathetic tone caused by abnormal sleep. Under these conditions, the central inhibition of overnight sympathetic tone could be a potential target for the treatment of chronic heart failure in terms of autonomic balancing.

This study was therefore designed to examine whether central sympathetic inhibition could restore normal sympathovagal balance during sleep in patients with chronic heart failure. Autonomic nervous function fluctuates in a parallel fashion with the REM/non-REM sleep cycle, so-called ultradian rhythm, in which parasympathetic tone is augmented particularly during non-REM sleep. These autonomic variations could be faithfully reflected by HR variation during sleep[5,6,10] To extract autonomic fluctuations related to sleep dynamics, we quantified the ultradian rhythm of the overnight high-frequency (HF) components of HR variability (HRV).

## Methods

*Subjects*

The present study group comprisee 14 patients with stable heart failure (11 men, 3 women, mean age 57±16 years) with left ventricular ejection fraction less than 40%, and 13 age-matched subjects with normal cardiac function (9 men, 4 women, mean age 61±17 years) (Table 1). The New York Heart Association functional class of the heart failure patients was I in 4, II in 5, and III in 5 patients; 5 patients had ischemic heart disease and 9 had dilated cardiomyopathy. Diuretics had been given to 10 patients, angiotensin-converting enzyme inhibitors or angiotensin-receptor antagonists to 12, digoxin to 5, and $\beta$-blocker to 3. All these medications were continued throughout the study. The control subjects had stable angina pectoris (9), post-

*(Received February 9, 2005; revised manuscript received June 6, 2005; accepted June 28, 2005)*

*The Second Department of Internal Medicine, Toyama Medical and Pharmaceutical University, Toyama, Japan*

Mailing address: Hidetsugu Asanoi, MD, The Second Department of Internal Medicine, Toyama Medical and Pharmaceutical University, 2630 Sugitani, Toyama 930-0194, Japan. E-mail: hidetugu@ms.toyama-mpu.ac.jp

**Table 1 Clinical Characteristics of the Study Group**

| | Normal cardiac function (n=13) | Chronic heart failure (n=14) | | |
|---|---|---|---|---|
| | | Baseline | Guanfacine | (%Change) |
| Age (years) | 61±17 | 57±16 | | |
| Body weight (kg) | 65±17 | 59±13 | 59±13 | (0±2) |
| During wakefulness | | | | |
| Mean HR (beats/min) | 64±8 | 75±10†† | 68±9* | (−10±9)** |
| Systolic BP (mmHg) | 117±9 | 111±13 | 105±12 | (−5±10)* |
| Diastolic BP (mmHg) | 69±12 | 68±10 | 68±9 | (−6±13)* |
| Mean BP (mmHg) | 85±10 | 82±9 | 77±9* | (−7±9)** |
| LVEDd (mm) | 44±4 | 62±10†† | 64±7 | (1±7) |
| LVEDs (mm) | 27±5 | 54±11†† | 57±9 | (1±7) |
| LVEF (%) | 70±9 | 26±10†† | 26±11 | (2±22) |
| CTR (%) | 48±6 | 54±6† | 54±7 | (0±5) |
| Urinary volume (ml/day) | 1,556±685 | 1,114±528 | 1,256±499 | (22±31) |
| BNP (pg/ml) | 20±13 | 152±140†† | 162±208 | (13±55) |
| NE (pg/ml) | 227±144 | 389±204 | 241±125* | (−34±33)** |
| PRA ($ng \cdot ml^{-1} \cdot h^{-1}$) | 2.5±1.9 | 8.8±7.0†† | 6.5±5.6 | (18±94) |
| PAC (pg/ml) | 9.4±6.9 | 17.0±14.6 | 9.9±5.1 | (−22±34)* |
| During sleep | | | | |
| Mean HR (beats/min) | 58±11 | 69±13† | 63±10* | (−8±9)** |
| Total power ($s^2$/Hz) | 0.5±0.5 | 0.04±0.03†† | 0.10±0.11 | (124±94)** |
| HF ($s^2$/Hz) | 0.2±0.2 | 0.02±0.02† | 0.04±0.05 | (154±164)** |
| LF/HF ratio | 2.9±2.0 | 2.0±1.6 | 1.7±2.0 | (−16±40) |
| Ultradian power of HF ($HF^2$/Hz) | 0.4±0.6 | 0.01±0.02†† | 0.04±0.06 | (361±239)** |

*Values are mean±SD. HR, heart rate; BP, blood pressure; LVEDd, left ventricular end-diastolic diameter; LVEDs, left ventricular end-systolic diameter; LVEF, left ventricular ejection fraction; CTR, cardiothoracic ratio; BNP, plasma brain natriuretic peptide concentration; NE, plasma norepinephrine concentration; PRA, plasma renin activity; PAC, plasma aldosterone concentration; HF, high-frequency power; LF, low-frequency power.*
*†p<0.05, ††p<0.01 Normal vs Baseline. *p<0.05, **p<0.01 Baseline vs Guanfacine.*

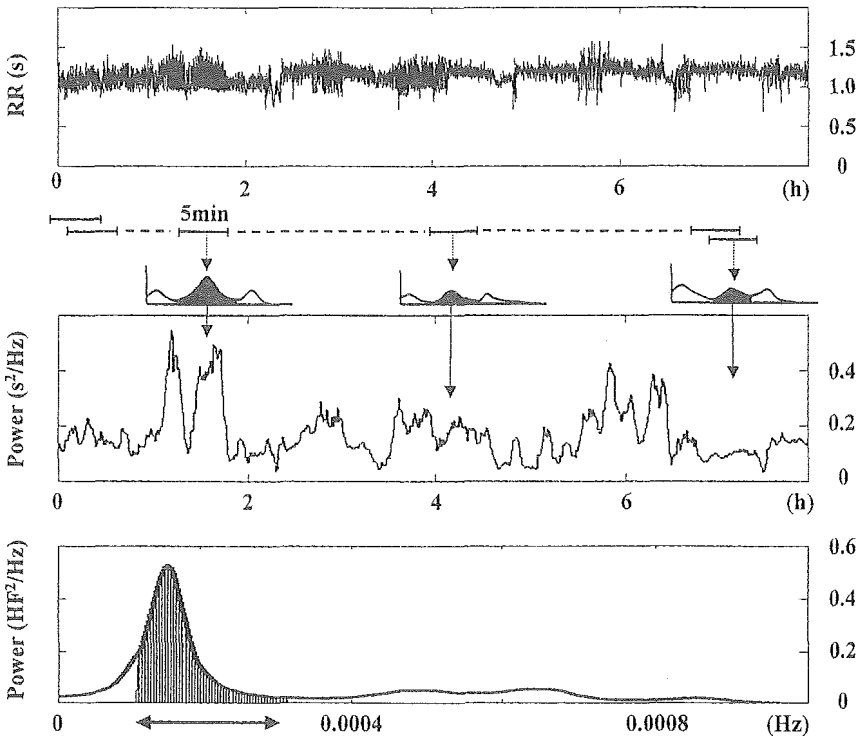


Fig 1. All-night spectral analysis of heart rate variability and ultradian power derived from high-frequency components in a representative subject with normal cardiac function. High-frequency spectral band (shaded area: 0.12–0.5 Hz) of sequential 5-min RR intervals was traced every 50 s, as shown in the middle panel. The bottom panel shows the sleep-related ultradian rhythm of all-night high-frequency component variability (arrow: 0.0001–0.0003 Hz).

myocarditis (1), paroxysmal supraventricular tachycardia (1) or mild hypertension (2). None had lung disorders, atrial fibrillation, anemia, severe hypoxemia (partial pressure of arterial oxygen <80 mmHg), diabetes mellitus, or autonomic failure of other origin. Written informed consent was given by all patients and the study was approved by the Institutional Human Subjects Review Committee.

*Study Protocol*

In all patients, overnight electrocardiography (ECG) without polysomnography was performed for serial power spectral analyses of HRV. The next morning a resting blood sample was obtained after 30 min supine rest for measurements of plasma norepinephrine (NE), brain natriuretic peptide (BNP), and aldosterone concentrations, and

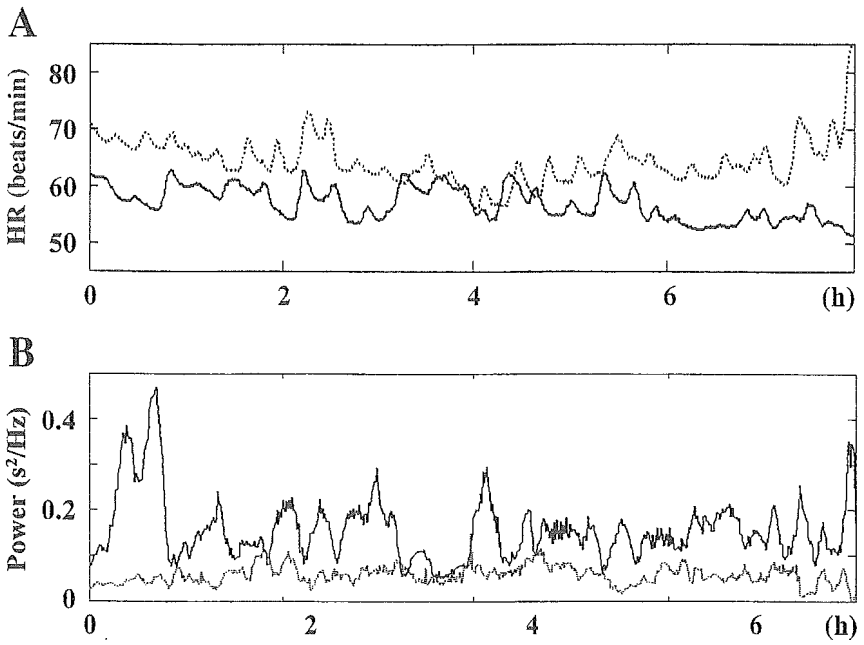


Fig 2. Overnight profile of heart rate (HR) and the spectral power of high-frequency (HF) components of heart rate variability in a patient with chronic heart failure from dilated cardiomyopathy. After administration of guanfacine (solid lines), all-night HR decreased with a concomitant increase in fluctuating HF power compared with the baseline before guanfacine (dotted lines).

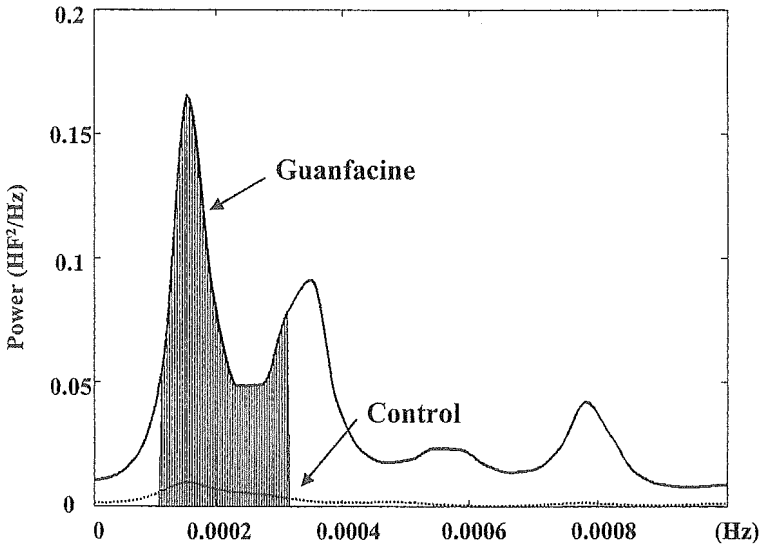


Fig 3. Ultradian power of all-night high-frequency (HF)-component variability in the same patient as in Fig 2. Guanfacine augmented the ultradian power markedly compared with that of control before guanfacine. Shaded area indicates the ultradian power corresponding to the frequency range 0.0001–0.0003 Hz of the rapid-eye movement (REM)/non-REM sleep cycle.

plasma renin activity. Then, the 14 patients with heart failure were given low-dose guanfacine (0.25 mg), an $\alpha_2$-adrenergic agonist, once daily before sleep as previously reported[11,12] After a 5-day regimen, the same measurements were repeated. Changes in cardiac size and function were also examined by chest radiography and 2-dimensional (D) echocardiography before and after the treatment.

*Overnight Power Spectral Analysis of HRV*

ECG signals were recorded with a Holter ECG device (Morpheus, Teijin, Tokyo, Japan) at a sampling frequency of 256 Hz and stored in a memory disk.[13] The beat-by-beat RR interval was identified from each beat and resampled at 4 Hz to produce the same time series as described previously.[14–16] Across the entire sleep period, spectral analysis with maximum entropy method was applied to sequential 5-min RR intervals every 50 s to evaluate the spectral components of RR-interval variability: the low-frequency components (low-frequency power (LF), 0.04–0.12 Hz), HF components (HF, 0.12–0.5 Hz), total spectral power, and LF/HF. Fig 1 shows the all-night trend in the RR intervals and HF-component variability sampled at 0.02 Hz (every 50 s) in a control subject. Because the ultradian rhythm of REM/non-REM sleep cycle examined in our previous study[13] had nearly 90-min interval (0.00018±0.0001 Hz), we again applied the maximum entropy method to the HF components of HRV to extract the oscillatory components ranging from 0.0001 to 0.0003 Hz (Fig 1). We then quantified the sleep-related parasympathetic oscillation by the spectral power of HF components variability within these spectral ranges (ultradian power).

*Statistical Analysis*

All data are expressed as mean ± standard deviation. Baseline variables in controls and patients with heart failure were compared using an unpaired t-test. Differences in variables between before and after administration of guanfacine were examined with a paired t-test. The level of statistical

significance was set at $p<0.05$.

## Results

Baseline hemodynamic and autonomic variables and effects of guanfacine are summarized in Table 1. Resting BNP and averaged all-night HR were significantly higher in patients with heart failure than in control subjects. All-night spectral power of HRV and the ultradian power of HF-component variability were markedly decreased in patients with heart failure. These patients tolerated guanfacine without adverse effects. The 5-day therapy regimen decreased HR, blood pressure, plasma NE and aldosterone concentrations significantly, but did not change left ventricular function, plasma BNP concentration or urinary output.

Fig 2 shows the all-night profiles in HR and the HF components of HRV before and after treatment with guanfacine in a patient with dilated cardiomyopathy. Guanfacine significantly increased all spectral power, especially that of the HF components. However, a resultant decline in LF/HF did not reach statistical significance. The augmentation of HF components was accompanied by predominant overnight fluctuations that were reflected by a selective augmentation of the ultradian spectral power of HF-component variability (Fig 3). Although average changes in spectral components did not reach statistical significance because of inter-individual variations of the baseline data, relative changes in total power, HF power, and the ultradian power of all-night HF-component variability were highly significant (Table 1).

## Discussion

In the present study night-time HRV in patients with heart failure was characterized by an attenuated ultradian rhythm of HF-components with a concomitant reduction in the averaged power of the HF- and LF-components. Low-dose guanfacine restored the nocturnal autonomic imbalance toward parasympathetic predominance over sympathetic tone in these patients. The improvement of the autonomic function was manifested by a significant augmentation of all-night HF power of HRV in association with a concomitant reduction in blood pressure, HR, and plasma NE concentration the next morning. These favorable autonomic effects of guanfacine were likely achieved through its direct action of central sympathoinhibition, not through hemodynamic improvements, because cardiac function and BNP remained unchanged. Another important finding of the present study is the augmentation of sleep ultradian power of HF-component variability with guanfacine, which suggests that the magnitude of the REM/non-REM sleep rhythm was augmented by the central sympathetic inhibition.

*Effect of Low-Dose Guanfacine*

A parallel decline in blood pressure and plasma NE concentration suggests that the sympathetic baroreflex function was reset toward the lower pressure range by guanfacine. These explanation is derived from the experimental evidence that $\alpha 2$-adrenergic agonists are known to not only suppress sympathetic activity but also to enhance baroreflex function[17,18] The guanfacine-induced increase in parasympathetic tone could be mediated through an improved cardiopulmonary and arterial baroreceptor function, which is frequently observed in mild to moderate congestive heart failure[19,20] However, an $\alpha$-adrenergic agonist, clonidine, is known to augment barorereflexes through the central nervous system. In the MOXICON trial, there was an excess of deaths in patients treated with 1.5 mg moxonidine[21,22] which exerts a central sympathoinhibitory action through stimulation of imidazoline receptors. Although that dose of moxonidine was accompanied by 52% reduction in plasma NE concentrations[22] the actual central sympathoinhibitory effect could be more potent than reflected by the plasma NE concentration[12] Therefore, the doses of moxonidine for some patients could have been inappropriately sympathoablative, leading to insufficient cardiac support by residual sympathetic outflow[21,23] and progressive pump failure. We have documented previously that a small dose of guanfacine exerts sufficient but safe sympathoinhibition with augmentation of parasympathetic tone in patients with heart failure[11,12] Therefore, these effects of low-dose guanfacine have potential benefit to the failing heart and provide a rational basis for a novel therapeutic option for chronic heart failure.

*Autonomic Function Related to Ultradian Sleep Rhythm*

There have been several observations that autonomic function is synchronized with REM/non-REM ultradian sleep rhythm[24–27] Instantaneous HRV evaluated with Poincare plots documented that interbeat HRV reached the highest level in a parallel fashion with an increase in delta wave activity during non-REM sleep[24,27] Bonnet et al also demonstrated in normal subjects that the HRV of Stage 2 sleep containing electroencephalographic arousal resulted in a 35% reduction in HF power and an 89% increase in LF power as compared with Stage 2 without arousal[28] These findings suggest that HRV operates as a function of sleep stage within the context of the REM/non-REM sleep cycle and arousal or sleep disturbance. In the present study, therefore, we applied spectral analysis for the first time to the HF-component variability to quantify the sleep-related ultradian rhythm of parasympathetic tone in patients with heart failure. The enhancement of the ultradian power observed after the treatment with guanfacine probably indicates that central sympathetic inhibition increased the ultradian rhythm of delta wave non-REM sleep, a finding suggestive of an improvement in sleep quality.

*Study Limitations*

First, this study was limited by its open-label design, the small number of patients, and the lack of placebo control. However, factors other than guanfacine could little affect the present results, if at all, because the changes in the hemodynamic and autonomic balance after guanfacine were so consistent and significant. Second, although guanfacine suppresses sympathetic nerve activity largely through its stimulation of central $\alpha 2$ adrenergic receptors, the present results cannot exclude the possibility that inhibition of cardiac neuronal NE release by guanfacine restored the parasympathetic tone in patients with heart failure[29,30] Third, we did not perform polysomnography for assessment of sleep quality, because this study was focused on the autonomic rhythmicity during sleep and the power of autonomic balancing of central sympathoinhibition. Direct comparison between the dynamics of delta wave activity and the ultradian rhythm of HF-component variability is warranted to confirm the feasibility of the ultradian rhythm derived from HRV as a marker of sleep quality. Fourth, we have not examined the reproducibility of parasympathetic oscillation related to sleep stage. This could be

of some importance in interpreting the present results but is unlikely to be of major significance because hemodynamic, hormonal, and autonomic function showed similar directional changes with guanfacine. Finally, application of the maximum entropy method to all-night HF-component variability might result in a modest error because of the non-steady characteristics of REM/non-REM sleep cycles. Normally, slow wave oscillations with ultradian rhythm become prominent for the first 4 h of sleep and gradually decline towards the morning. To describe these sleep and autonomic profiles more precisely, spectral estimation based on the discrete wavelet transform should have been used. The wavelet distribution could provide beat-to-beat spectral analysis and illustrate transitional spectral changes within the 3-D framework of power, time, and frequency[14,16]

## Conclusions

The present study documented that central sympathetic inhibition with an $\alpha_2$-aderanergic agonist, guanfacine, augmented the sleep-related ultradian rhythm of parasympathetic tone in patients with chronic heart failure. The augmentation of the parasympathetic oscillatory tone during sleep is indicative of an improvement in sleep quality in these patients. Because sleep is a continuous oscillatory process, quantitative assessment of all-night ultradian dynamics of HRV serves as a useful tool to gain insight into the pathophysiologic interaction between the sleep process and autonomic function.

## References


1. Cohn JN, Levine TB, Olivari MT, Garberg V, Lura D, Francis GS, et al. Plasma norepinephrine as a guide to prognosis in patients with chronic congestive heart failure. *N Engl J Med* 1984; **311:** 819–823.
2. Lang CC, Rayos GH, Chomsky DB, Wood AJJ, Wilson JR. Effect of sympathoinhibition on exercise performance in patients with heart failure. *Circulation* 1997; **96:** 238–245.
3. Bradley TD, Floras JS. Pathophysiologic and therapeutic implications of sleep apnea in congestive heart failure. *J Card Fail* 1996; **2:** 223–240.
4. Banno K, Shiomi T, Sasanabe R, Otake K, Hasegawa R, Maekawa M, et al. Sleep-disordered breathing in patients with idiopathic cardiomyopathy. *Circ J* 2004; **68:** 338–342.
5. Okada H, Iwase S, Mano T, Sugiyama Y, Watanabe T. Changes in muscle sympathetic nerve activity during sleep in humans. *Neurology* 1991; **41:** 1961–1966.
6. Somers VK, Phil D, Dyken ME, Mark AL, Abboud FM. Sympathetic-nerve activity during sleep in normal subjects. *N Engl J Med* 1993; **328:** 303–307.
7. Casolo G, Balli E, Taddei T, Amuhasi J, Gori C. Decreased spontaneous heart rate variability in congestive heart failure. *Am J Cardiol* 1989; **15:** 1162–1167.
8. Joel DE, Timithy C, Sonia A, Paul M, Jack C, Michael ZG. Sympathetic nervous system alternations in sleep apnea: The relative importance of respiratory disturbance, hypoxia, and sleep quality. *Chest* 1997; **111:** 639–642.
9. Yasuma F, Nomura H, Hayashi H, Okada T, Tsuzuki M. Breathing abnormalities during sleep in patients with chronic heart failure. *Jpn Circ J* 1989; **53:** 1506–1510.
10. Vanoli E, Adamson PB, Ba-Lin GD, Lazzara R, Orr WC. Heart rate variability during specific sleep stages: A comparison of healthy subjects with patients after myocardial infarction. *Circulation* 1995; **91:** 1918–1922.
11. Yamada K, Asanoi H, Ueno H, Joho S, Takagawa J, Kameyama T, et al. Role of sympathoexcitation in enhanced hypercapnic chemosensitivity in patients with heart failure. *Am Heart J* 2004; **148:** 964–970.
12. Oda Y, Asanoi H, Ueno H, Yamada K, Joho S, Kameyama T, et al. Pulse-synchronous sympathetic burst power as a new index of sympathoexcitation in patients with heart failure. *Am J Physiol* 2004; **287:** H1821–H1827.
13. Yamazaki T, Asanoi H, Ueno H, Yamada K, Takagawa J, Kameyama T, et al. Circadian dynamics of heart rate and physical activity in patients with heart failure. *Clin Exp Hypertens* 2005; **2/3:** 241–249.
14. Joho S, Asanoi H, Remah HA, Igawa A, Kameyama T, Nozawa T, et al. Cardiac sympathetic denervation modulates the sympathoexcitatory response to acute myocardial ischemia. *J Am Coll Cardiol* 1999; **34:** 1924–1931.
15. Goso Y, Asanoi H, Ishise H, Kameyama T, Hirai T, Nozawa T, et al. Respiratory modulation of muscle sympathetic nerve activity in patients with chronic heart failure. *Circulation* 2001; **104:** 418–423.
16. Ueno H, Asanoi H, Yamada K, Oda Y, Takagawa J, Kameyama T, et al. Attenuated respiratory modulation of chemoreflex-mediated sympathoexcitation in patients with chronic heart failure. *J Card Fail* 2004; **10:** 236–243.
17. Korner PI, Oliver JR, Sleight P, Chalmers JP, Robinson JS. Effects of clonidine on the baroreceptor-heart rate reflex and on single aortic baroreceptor fibre discharge. *Eur J Pharmacol* 1974; **28:** 189–198.
18. Jens T, Jens J, Andre D, Michael O, Ralph P, Friedrich LC, et al. Clonidine improves spontaneous baroreflex sensitivity in conscious mice through parasympathetic activation. *Hypertension* 2004; **43:** 1042–1047.
19. Ishise H, Asanoi H, Ishizaka S, Joho S, Kameyama T, Umeno K, et al. Time course of sympathovagal imbalance and left ventricular dysfunction in conscious dogs with heart failure. *J Appl Physiol* 1998; **84:** 1234–1241.
20. Ferguson WD, Abbound FM, Mark AL. Selective impairment of baroreflex-mediated vasoconstrictor responses in patients with ventricular dysfunction. *Circulation* 1984; **69:** 451–460.
21. Coats AJ. Heart Failure 99: The Moxcon story. *Int J Cardiol* 1999; **71:** 109–111.
22. Swedberg K, Bristow MR, Cohn JN, Dargie H, Straub M, Wiltse C, et al. Effects of sustained-release moxonidine, an imidazoline agonist, on plasma norepinephrine in patients with chronic heart failure. *Circulation* 2002; **105:** 1797–1803.
23. Hermiller JB, Magorien RD, Leithe ME, Unverferth DV, Leier CV. Clonidine in congestive heart failure: A vasodilator with negative inotropic effects. *Am J Cardiol* 1983; **51:** 791–795.
24. Gronfier C, Simon C, Piquard F, Ehrhart J, Brandenberger G. Neuroendocrine processes underlying ultradian sleep regulation in man. *J Clin Endocrinol Metab* 1999; **84:** 2686–2690.
25. Baust W, Bohnert B. The regulation of heart rate during sleep. *Exp Brain Res* 1969; **7:** 169–180.
26. Baharav A, Kotagal S, Gibbons V, Rubin BK, Pratt G, Karin J, et al. Fluctuations in autonomic nervous activity during sleep displayed by power spectrum analysis of heart rate variability. *Neurology* 1995; **45:** 1183–1187.
27. Otzenberger H, Gronfier C, Simon C, Charloux A, Ehrhart J, Piquard F, et al. Dynamic heart rate variability: A tool for exploring sympathovagal balance continuously during sleep in men. *Am J Physiol* 1998; **275:** H946–H950.
28. Bonnet MH, Arand DL. Heart rate variability: Sleep stage, time of night, and arousal influences. *Electroencephalogr Clin Neurophysiol* 1997; **102:** 390–396.
29. Azevedo ER, Newton GE, Parker JD. Cardiac and systemic sympathetic activity in response to clonidine in human heart failure. *J Am Coll Cardiol* 1999; **33:** 186–191.
30. Azevedo ER, Parker JD. Parasympathetic control of cardiac sympathetic activity. *Circulation* 1999; **100:** 274–279.

# Repolarization Dynamics in Patients with Idiopathic Ventricular Fibrillation

## *Pharmacological Therapy with Bepridil and Disopyramide*

*Masataka Sugao, MD, Akira Fujiki, MD, Kunihiro Nishida, MD, Masao Sakabe, MD, Takayuki Tsuneda, MD, Jotaro Iwamoto, MD, Koichi Mizumaki, MD, and Hiroshi Inoue, MD*

**Abstract:** The electrocardiographic parameters relating occurrence of ventricular fibrillation (VF) episodes in patients with idiopathic VF (IVF) are still unknown. The aim of this study was to clarify efficacy of pharmacological therapy in patients with IVF with respect to repolarization dynamics. The study group consisted of 8 men (age 43.6 ± 9.1 years) with IVF (Brugada type 5 patients, prominent J wave in the inferior leads 3 patients) who had documented spontaneous episodes of VF, 7 of whom had implantable cardioverter defibrillators. The relation between QT and RR interval was analyzed from 24-hour Holter ECG using an automatic analyzing system before and after pharmacological therapy (bepridil 5 and disopyramide 3). From QT–RR linear regression lines, QT intervals were determined at RR intervals of 0.6 second [QT(0.6)], 1.0 second [QT(1.0)], and 1.2 seconds [QT(1.2)]. Pharmacological therapy increased the slope of QT–RR regression line from 0.105 ± 0.020 to 0.144 ± 0.037 ($P < 0.05$). Accordingly, QT(1.0) and QT(1.2) became longer after drug therapy [QT(1.0), 0.382 ± 0.016 seconds vs 0.414 ± 0.016 seconds ($P < 0.01$); QT(1.2), 0.403 ± 0.017 seconds vs 0.442 ± 0.021 seconds ($P < 0.01$)]. However, QT(0.6) did not change after drug administration. Before drug therapy the average episodes of VF were 5.5 ± 5.8 (range 1 to17) during the observation period of 19.3 ± 17.6 months (range 6 to 60 months). After drug therapy, 6 patients had no episode of VF for 24 to 120 months (66.0 ± 38.5 months). Two patients had a single episode of VF for 12- and 96-month follow-ups. Pharmacological therapy decreased the frequency of VF episodes in association with prolongation of QT intervals at slower heart rates. Not only J wave and ST elevation but also shorter QT intervals at slower heart rates may represent an electrophysiological substrate for development of VF episodes in these specific IVF patients.

**Key Words:** bepridil, Brugada syndrome, disopyramide, idiopathic ventricular fibrillation, QT interval

(*J Cardiovasc Pharmacol*™ 2005;45:545–549)

Idiopathic ventricular fibrillation (IVF) has been recognized as a cause of unexplained, nocturnal sudden death in middle-aged men, especially in Asian countries.[1,2] In some of these patients with IVF, high-takeoff ST-segment and prominent J wave in the right precordial leads have been reported.[3] Furthermore, IVF patients without this specific ECG pattern have been reported, and some of them have a prominent J wave in the inferior leads.[4] In these IVF patients, the most reliable therapy for prevention of sudden death is implantation of an implantable cardioverter defibrillator (ICD). However, frequent episodes of VF reduce quality of life because of frequent shock therapy from ICD. Recently, Belhassen et al reported that quinidine is effective for prevention of spontaneous episodes of VF in Brugada syndrome, but it was associated with a 36% incidence of side effects.[5] In IVF patients including Brugada and non-Brugada ECG patterns, we have found a lower slope of the QT–RR relation and shorter QT interval at slow heart rates compared with age-matched healthy subjects.[6] Hence, we evaluated efficacy of pharmacological therapy with antiarrhythmic drugs prolonging QT interval (bepridil and disopyramide) in patients with IVF with respect to the 24-hour QT–RR relationship.

## METHODS

### Subjects

The study group consisted of 8 men ranging in age from 33 to 53 years (43.6 ± 9.1 years) including 5 subjects with Brugada type and 3 subjects with non-Brugada type (prominent J wave in the inferior leads) who had documented spontaneous episodes of VF. All patients underwent physical examination, 12-lead ECG, 24-hour Holter ECG, treadmill exercise testing, and biochemical and hematological testing. None had a prolonged QT interval during the course of syncopal episodes or had cardiovascular disease including hypertension, coronary artery disease, or congestive heart disease. All IVF patients underwent implantation of an ICD except one patient, who had refused. After informed consent was obtained, patients were followed without pharmacological therapy at least 6 months, and then all patients received antiarrhythmic drug therapy (bepridil 200 mg/d or disopyramide 300 mg/d).

Received for publication December 24, 2004; accepted February 4, 2005.
From The Second Department of Internal Medicine, Toyama Medical and Pharmaceutical University, Toyama, Japan.
Reprints: Akira Fujiki, MD, The Second Department of Internal Medicine, Toyama Medical and Pharmaceutical University, 2630 Sugitani, Toyama, 930-0194, Japan (e-mail:fujiki@ms.toyama-mpu.ac.jp).

## Analysis of RR and QT Interval

QT and RR intervals were determined from 24-hour Holter ECG data within 2 weeks after VF episodes before drug administration, and during pharmacological therapy without VF episodes at least 6 months. Using an automatic measurement system (SCM6000 Fukuda Denshi, Tokyo, Japan), signal-averaged waves from CM5 lead were obtained by the summation of consecutive sinus beats during each 15-second period throughout 24 hours. The end of the T wave was determined automatically according to the following algorithm (HPS-QTM Fukuda Denshi, Tokyo, Japan). The top of the T wave was determined as the point where the first derivative (dv/dt) of the T wave changed from positive to negative. The endpoint of the T wave was determined as the point where the first derivative of the T wave became undetectable after the top of T wave. In each case, detection level of the first derivative of T wave was set as the average level of ST segment.

We confirmed the accuracy of the automatic measurement of QT intervals manually. For the averaged period of 15 seconds, a corresponding mean RR interval was calculated, and measured QT interval was plotted against the corresponding mean RR interval. For the analyses of the QT–RR relationship, a regression line was used, and QT at RR intervals of 0.6, 1.0, and 1.2 seconds were calculated.

## Statistics

Results are presented as mean ± SD. The dependence of QT interval on the RR interval was analyzed by linear regression using the entire 24-hour tracing in each patient (QT = A[RR] + B, where A is the slope and B is the intercept). The differences in continuous variables between groups were analyzed by Student *t* test for paired and unpaired data. Statistical significance was set at $P < 0.05$.

# RESULTS

## QT–RR Relation Before and After Pharmacological Therapy

Representative 12-lead ECG recordings and QT–RR relations from a Brugada type IVF patient before and after bepridil therapy (200 mg/d) are shown in Figures 1 and 2. After bepridil treatment, the slope of QT–RR regression line became steeper compared with control state.

Values of slope and intercept of QT–RR linear regression lines and QT intervals at preselected RR intervals for each IVF patient before and after pharmacological therapy are summarized in Tables 1 and 2. Bepridil and disopyramide increased the slope of QT–RR relations from 0.105 ± 0.020 to 0.144 ± 0.037 ($P < 0.05$). Drug administration also increased QT intervals at RR intervals of 1.0 second and 1.2 seconds [QT(1.0), 0.382 ± 0.016 seconds vs 0.414 ± 0.016 seconds, $P < 0.01$; QT(1.2), 0.403 ± 0.017 seconds vs 0.442 ± 0.021 seconds, $P < 0.01$]. However, QT at an RR interval of 0.6 second did not change with drug administration.

## Follow-up With Bepridil and Disopyramide

Effects of pharmacological therapy on VF episodes are summarized in Table 3. Before drug therapy, the average observation period was 19.3 ± 17.6 months (range 6 to 60 months), and the average episodes of VF were 5.5 ± 5.8 (range 1 to 17). All patients received either bepridil or disopyramide for 52.5 ± 41.0 months (range 12 to 120 months). Six patients had no episode of VF for 24 to 120 months (66.0 ± 38.5 months). However, 2 patients had a single VF episode treated with ICD. The first patient (case 1) with Brugada syndrome had 17 episodes of VF during a 28-month follow-up period before drug therapy, and he suffered from frequent ICD shocks. After starting bepridil (200 mg/d), he had only 1 episode of VF during 12 months of follow-up. The second patient (case 7) with J wave elevation in the inferior leads had 11 nocturnal

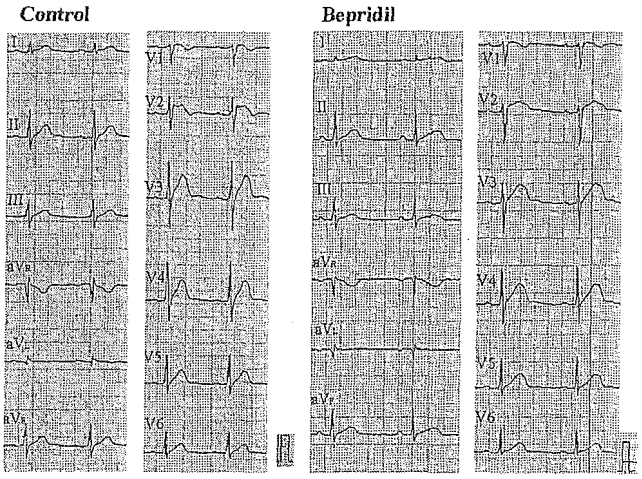


**FIGURE 1.** Twelve-lead electrocardiogram in a patient with Brugada syndrome before and after pharmacological therapy with bepridil (case 4). Before drug therapy, saddleback type ST segment elevation was seen in V2, and QT interval in V5 was 0.34 second. After bepridil (200 mg/d) administration for 12 months, QT interval increased to 0.40 second, and J wave elevation in V2 was suppressed, but late component of ST segment increased.

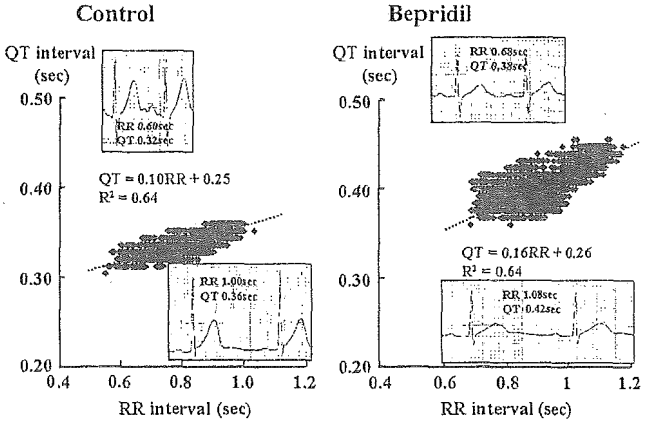


**FIGURE 2.** QT–RR relationship in a patient with Brugada syndrome before and after pharmacological therapy with bepridil (the same patient as in Figure 1). The slope of the QT–RR regression line before drug therapy was lower than that after bepridil therapy.

TABLE 1. QT–RR Relation and QT Intervals in Idiopathic Ventricular Fibrillation (IVF) Before Drug Therapy

| | | QT–RR Relation | | QT Interval (Seconds) | | |
|---|---|---|---|---|---|---|
| Case No. | Age (Years) | Slope | Intercept | RR 0.6 s | RR 1.0 s | RR 1.2 s |
| 1* | 35 | 0.132 | 0.246 | 0.325 | 0.378 | 0.405 |
| 2* | 53 | 0.097 | 0.287 | 0.345 | 0.384 | 0.404 |
| 3* | 53 | 0.080 | 0.308 | 0.356 | 0.388 | 0.404 |
| 4* | 49 | 0.101 | 0.253 | 0.314 | 0.354 | 0.374 |
| 5 | 33 | 0.097 | 0.272 | 0.330 | 0.369 | 0.388 |
| 6* | 52 | 0.104 | 0.278 | 0.341 | 0.383 | 0.404 |
| 7 | 41 | 0.093 | 0.315 | 0.370 | 0.408 | 0.426 |
| 8 | 33 | 0.138 | 0.257 | 0.340 | 0.395 | 0.423 |
| Average | 43.6 | 0.105 | 0.277 | 0.340 | 0.382 | 0.403 |
| SD | 9.1 | 0.020 | 0.025 | 0.018 | 0.016 | 0.017 |

*Brugada syndrome.

TABLE 3. Effects of Bepridil and Disopyramide on Episodes of Ventricular Fibrillation (VF)

| | | Before Drug Therapy | | After Drug Therapy | |
|---|---|---|---|---|---|
| Case No. | ICD Implantation | Episodes of VF | Observation Period (Months) | Episodes of VF | Observation Period (Months) |
| 1* | (+) | 17 | 28 | 1 | 12 |
| 2* | (+) | 2 | 12 | 0 | 72 |
| 3* | (+) | 1 | 12 | 0 | 12 |
| 4* | (+) | 2 | 12 | 0 | 24 |
| 5 | (+) | 2 | 12 | 0 | 24 |
| 6* | (+) | 7 | 12 | 0 | 60 |
| 7 | (+) | 11 | 60 | 1 | 96 |
| 8 | (−) | 2 | 6 | 0 | 120 |
| Average | | 5.5 | 19.3 | 0.3 | 52.5 |
| SD | | 5.8 | 17.6 | 0.5 | 41.0 |

ICD, implantable cardioverter defibrillator.
*Brugada syndrome.

episodes of VF before drug administration. During 96 months of follow-up after starting disopyramide (300 mg/d), he had only 1 episode of VF treated with ICD. No adverse effect of drug administration was observed during follow-up periods.

## DISCUSSION

The major findings of the present study were as follows: (1) Pharmacological therapy with bepridil and disopyramide significantly reduced frequency of VF episodes in patients with prominent J wave and ST segment elevation. (2) In patients with IVF who had had recent VF episodes, the slope of QT–RR regression line was lower, and QT intervals at RR intervals of 1.0 and 1.2 seconds were shorter than those obtained after successful treatment with bepridil and disopyramide for at least 6 months. These results suggest that failure of prolongation of QT interval (shorter QT interval) at slower heart rates may play an important role for spontaneous occurrence of VF episodes,[6,7] and both bepridil and disopyramide are effective for reducing frequency of VF episodes through modification of repolarization dynamics.

TABLE 2. QT–RR Relation and QT Intervals in Idiopathic Ventricular Fibrillation (IVF) After Drug Therapy

| | | QT–RR Relation | | QT Interval (Seconds) | | |
|---|---|---|---|---|---|---|
| Case No. | Antiarrhythmic Drugs | Slope | Intercept | RR 0.6 s | RR 1.0 s | RR 1.2 s |
| 1* | Bepridil | 0.132 | 0.290 | 0.369 | 0.422 | 0.449 |
| 2* | Bepridil | 0.096 | 0.312 | 0.369 | 0.408 | 0.427 |
| 3* | Bepridil | 0.159 | 0.270 | 0.366 | 0.429 | 0.461 |
| 4* | Bepridil | 0.156 | 0.264 | 0.358 | 0.420 | 0.451 |
| 5 | Bepridil | 0.099 | 0.295 | 0.354 | 0.394 | 0.414 |
| 6* | Disopyramide | 0.204 | 0.233 | 0.356 | 0.438 | 0.479 |
| 7 | Disopyramide | 0.132 | 0.263 | 0.342 | 0.395 | 0.422 |
| 8 | Disopyramide | 0.176 | 0.230 | 0.336 | 0.406 | 0.441 |
| Average | | 0.144† | 0.270 | 0.357 | 0.414‡ | 0.442‡ |
| SD | | 0.037 | 0.029 | 0.012 | 0.016 | 0.021 |

*Brugada syndrome; †$P < 0.05$ and ‡$P < 0.01$ vs before drug therapy.

## Repolarization Dynamics in IVF Patients

In our previous study, we analyzed Holter ECGs recorded just after VF episodes and found that IVF patients had lower slopes of the QT–RR relation and impaired prolongation of QT interval at longer RR intervals compared with control healthy subjects.[6] It is possible that repolarization dynamics in patients with IVF might be variable depending on pharmacological therapy. Hence, in the present study, we determined QT–RR relations before and after antiarrhythmic drug therapy.

Our observations indicate that IVF patients with episodes of VF may have unique repolarization dynamics, ie, impaired prolongation of QT intervals at longer RR intervals.[6,7] Smaller QT prolongation at longer RR intervals results in a lower slope of the QT–RR relation. These repolarization characteristics in IVF patients during sinus bradycardia may be related to the nocturnal occurrence of VF episodes.[2] Both bepridil and disopyramide increased the slope of the QT–RR relation along with prolongation of QT interval and successfully suppressed VF episode.

Although the mechanism of VF is still unclear, and heterogeneity of mechanisms may contribute to differences in ECG features in patients with IVF, these patients have a prominent J wave and ST elevation in either the precordial or the inferior leads. In the present study, IVF patients without Brugada-like ECG showed a similar relationship of QT with RR intervals as patients with Brugada type ECG. It is therefore possible that a combination of characteristic J wave and ST elevation with abnormal repolarization dynamics could reflect a common underlying mechanism in IVF patients irrespective of the site of ECG leads having a specific J wave or ST segment elevation pattern.

## Mechanism of Lower Slope of QT–RR Relation and Short QT Interval at Slower Heart Rates

Recent studies suggested that the presence of a prominent transient outward current ($I_{to}$) in the right ventricular epicardial layer and genetic abnormalities of the sodium channel gene (SCN5A) may play a key role in the characteristic ECG pattern in Brugada syndrome.[8–10] Experiments using wedge preparations of canine heart revealed that a down-sloping ST-segment elevation may be caused by an earlier repolarization of the epicardial action potential because of a more intense $I_{to}$.[11,12] Na channel blocking agents induced a coved type of ST elevation in the precordial leads[13] because they accentuated $I_{to}$-mediated notch and failed to develop the action potential plateau (loss of dome). We hypothesized that these abnormalities of ionic currents might affect not only configuration of ST segment pattern but also ventricular repolarization dynamics.

Either reduction of inward currents ($I_{Na}$ or $I_{Ca}$) or increase in outward currents ($I_K$ or $I_{to}$) causes early repolarization, resulting in shortening of the QT interval. At rest, an increase in $I_{to}$ may limit the prolongation of action potential duration, especially at slower heart rates, and also produce prominent J wave in surface ECG. During exercise, both faster heart rates and an increase in adrenergic tone may offset the excessive $I_{to}$ current[14] and make a difference in QT interval at higher heart rates (for instance, RR interval of 0.6 seconds) insignificant compared with healthy subjects.

## Bepridil and Disopyramide

Bepridil hydrochloride, a diarylaminopropylamine derivative, was introduced as a Ca antagonist affecting both L and T type Ca channels with a lidocaine-like fast kinetic block of Na current.[15] Bepridil also has unique electrophysiological properties to inhibit outward currents including most types of K current ($I_{Kr}$, $I_{Ks}$, $I_{Kur}$, $I_{K1}$, $I_{KACh}$, $I_{KATP}$) and $I_{to}$.[16] In Figure 1, bepridil prolonged QT interval and decreased J wave amplitude in $V_2$ but increased the late component of the ST segment. Disopyramide possesses intermediate kinetics of Na channel blocking effect and suppresses several types of K current ($I_{Kr}$, $I_{KACh}$, $I_{KATP}$) and $I_{to}$.[17] Both drugs increased the slopes of QT–RR regression lines and reduced frequency of spontaneous VF episodes in the present study. Suppression of not only $I_{to}$ but also other K channels may contribute to prolongation of QT interval in IVF patients and benefit for prevention of VF episodes. The prolonged QT interval at RR intervals of 1.0 second and 1.2 seconds after drug therapy became similar to the values in the healthy controls in our previous paper.[6] The underlying mechanisms of effects of multichannel blocking drugs on suppression of phase 2 reentry should be investigated further.[18] Although bepridil and disopyramide are effective in decreasing VF episodes in IVF patients, the most reliable therapy for prevention of sudden death is ICD. These antiarrhythmic drugs may improve quality of life after ICD implantation through decreasing frequency of shock therapy.

## Study Limitations

In the present study, the number of IVF patients was small, and ECG patterns were heterogeneous: 5 patients had Brugada-type and 3 had non-Brugada-type ECG. However, they showed the similar repolarization abnormality, a finding suggesting the presence of a common underlying electrophysiological abnormality. In patients with Brugada type ECG, precordial leads close to the anterior right ventricular wall may be appropriate for the measurement of QT intervals, but we analyzed QT in CM5 lead because of higher reliability of automatic QT measurement. Abnormality in ventricular repolarization dynamics observed in CM5 lead suggests that not only the J wave and ST segment elevation but also the abnormal relationship of QT with RR may be useful for evaluation of efficacy of antiarrhythmic drugs. Although cardioversion of VF in itself may affect the repolarization pattern, Holter ECG recordings were done at least a few days after an episode of VF, and we believe it is quite unlikely. The unique repolarization dynamics in IVF may be regulated by several other factors including autonomic nervous system, electrolyte balance, and glucose-induced insulin secretion[19] and may contribute to spontaneous onset of VF episodes. The relation between these factors and repolarization dynamics in IVF patients should be evaluated further.

## REFERENCES


1. Viskin S, Belhassen B. Idiopathic ventricular fibrillation. *Am Heart J.* 1990;120:661–671.
2. Nademanee K, Veerakul G, Nimmannit S, et al. Arrhythmogenic marker for the sudden unexplained death syndrome in Thai men. *Circulation.* 1997;96:2595–2600.
3. Brugada P, Brugada J. Right bundle-branch block, persistent ST segment elevation and sudden cardiac death: a distinct clinical and electrocardiographic syndrome. A muticenter report. *J Am Coll Cardiol.* 1992;20:1391–1396.
4. Kalla H, Yan GX, Marinchak R. Ventricular fibrillation in a patient with prominent J (Osborn) waves and ST segment elevation in the inferior electrocardiographic leads: a Brugada syndrome variant? *J Cardiovasc Electrophysiol.* 2000;11:95–98.
5. Belhassen B, Glick A, Vislin S. Efficacy of quinidine in high-risk patients with Brugada syndrome. *Circulation.* 2004;110:1731–1737.
6. Fujiki A, Sugao M, Nishida K, et al. Repolarization abnormality in idiopathic ventricular fibrillation: assessment using 24-hour QT–RR and QaT–RR relationships. *J Cardiovasc Electrophysiol.* 2004;15:59–63.
7. Viskin S, Zeltser D, Ish-Shalom M, et al. Is idiopathic ventricular fibrillation a short QT syndrome? Comparison of QT intervals of patients with idiopathic ventricular fibrillation and healthy controls. *Heart Rhythm.* 2004;1:587–591.
8. Chen Q, Kirsch GE, Zhang D, et al. Genetic basis and molecular mechanism for idiopathic ventricular fibrillation. *Nature.* 1998;392:293–296.
9. Gussak I, Antzelevitch C, Bjerregaard P, et al. The Brugada syndrome: clinical, electrophysiologic and genetic aspects. *J Am Coll Cardiol.* 1999;33:5–15.
10. Smits JP, Eckardt L, Probst V, et al. Genotype–phenotype relationship in Brugada syndrome: electrocardiographic features differentiate SCN5A-related patients from non-SCN5A-related patients. *J Am Coll Cardiol.* 2002;40:350–356.
11. Di Diego JM, Sun ZQ, Antzelevitch C. $I_{to}$ and action potential notch are smaller in left vs. right ventricular epicardium. *Am J Physiol.* 1996;271:H548–H561.
12. Yan GX, Antzelevitch C. Cellular basis for the Brugada syndrome and other mechanisms of arrhythmogenesis associated with ST-segment elevation. *Circulation.* 1999;100:1660–1666.
13. Fujiki A, Usui M, Nagasawa H, et al. ST segment elevation in the right precordial leads induced with class Ic antiarrhythmic drugs: insight into the mechanism of Brugada syndrome. *J Cardiovasc Electrophysiol.* 1999;10:214–218.
14. Litovsky SH, Antzelevitch C. Differences in the electrophysiological response of canine ventricular subendocardium and subepicardium to

acetylcholine and isoproterenol. A direct effect of acetylcholine in ventricular myocardium. *Circ Res.* 1990;67:615–627.
15. Anno T, Furuta T, Itho M, et al. Effects of bepridil on the electrophysiological properties of guinea-pig ventricular muscles. *Br J Pharmacol.* 1984;81:589–597.
16. Berger F, Borchard U, Hafner D. Effects of the calcium entry blocker bepridil on repolarizing and pacemaker currents in sheep cardiac Purkinje fibres. *Naunyn Schmiedebergs Arch Pharmacol.* 1989;339:638–646.
17. Coraboeuf E, Deroubaix E, Escande D, et al. Comparative effects of three class I antiarrhythmic drugs on plateau and pacemaker currents of sheep cardiac Purkinje fibers. *Cardiovasc Res.* 1988;22:375–384.
18. Miyoshi S, Mitamura H, Fujikura K, et al. A mathematical model of phase 2 reentry: role of L-type Ca current. *Am J Physiol Heart Circ Physiol.* 2003;284:H1285–H1294.
19. Nishizaki M, Sakurada H, Ashikaga T, et al. Effects of glucose-induced insulin secretion on ST segment elevation in the Brugada syndrome. *J Cardiovasc Electrophysiol.* 2003;14:243–249.

# Ischemia-Induced Norepinephrine Release, but not Norepinephrine-Derived Free Radicals, Contributes to Myocardial Ischemia–Reperfusion Injury

Makoto Nonomura, MD; Takashi Nozawa, MD; Akira Matsuki, MD; Teruo Nakadate, MD; Norio Igarashi, MD; Bun-ichi Kato, MD; Nozomu Fujii, MD; Akihiko Igawa, MD; Hidetsugu Asanoi, MD; Takashi Kondo, PhD; Hiroshi Inoue, MD

Circulation Journal
Vol. 69 No. 5 May 2005
(Pages 590–595)

*Circ J* 2005; **69:** 590–595

# Ischemia-Induced Norepinephrine Release, but not Norepinephrine-Derived Free Radicals, Contributes to Myocardial Ischemia–Reperfusion Injury

Makoto Nonomura, MD; Takashi Nozawa, MD; Akira Matsuki, MD; Teruo Nakadate, MD; Norio Igarashi, MD; Bun-ichi Kato, MD; Nozomu Fujii, MD; Akihiko Igawa, MD; Hidetsugu Asanoi, MD; Takashi Kondo, PhD*; Hiroshi Inoue, MD

**Background** Norepinephrine (NE)-derived free radicals may contribute to myocyte injury after ischemia–reperfusion, so the influence of sympathetic denervation on myocardial ischemia–reperfusion injury was investigated in the present study.

**Methods and Results** Cardiac sympathetic denervation was produced in Wistar rats by a solution of 10% phenol 1 week before ischemia. Atenolol (0.5 mg/kg) was intravenously administered 10 min before the coronary occlusion. The left coronary artery was occluded for 30 min and thereafter reperfused. Cardiac interstitial fluid was collected by a microdialysis probe and free radicals in dialysate were determined by electron paramagnetic resonance (EPR) spin trapping, using 5,5-dimethyl-1-pyrroline-N-oxide as a spin trap. The ratio of infarct size to the ischemic area at risk (I/R) was decreased in both the phenol and atenolol groups compared with control (28.5±11.3, 31.8±10.7 vs 50.6±14.7%, $p<0.05$). During the coronary occlusion, concentrations of interstitial NE increased markedly in the control and atenolol groups, but was unchanged in the phenol group. EPR signal intensity (relative value to internal standard) was maximal at 1 h after reperfusion and was similar in the phenol and control groups (0.32±0.15 vs 0.45±0.19).

**Conclusions** Cardiac denervation protected myocyte against ischemia–reperfusion injury through decreasing direct NE toxicity, but not through decreasing NE-derived free radicals. (*Circ J* 2005; **69:** 590–595)

**Key Words:** β-blocker; Electron paramagnetic resonance; Rat; Sympathetic denervation

It is generally accepted that excess levels of norepinephrine (NE) could lead to myocardial injury[1–4] Prolonged myocardial ischemia causes a large amount of NE to be released from the sympathetic nerve terminals via non-exocytotic local metabolic mechanism independently of central sympathetic activation, and this excessive NE may promote myocardial injury[5] Reperfusion following prolonged ischemia would prevent progression of ischemic cell necrosis, whereas reperfusion itself causes myocardial injury, the phenomenon known as reperfusion injury[6–10] Increased interstitial concentration of NE during ischemia may be involved in the pathogenesis of reperfusion injury, because NE is a source of free radicals[11–13] Previous studies have shown that auto-oxidation of NE results in the generation of highly reactive ·OH radicals[12,13] Thus, the pathogenesis of catecholamine-induced myocardial injury in the setting of reperfusion following prolonged ischemia is multifactorial, but the relative role of this NE-derived free radical formation in increasing the size of the infarct after reperfusion remains unclear. Accordingly, we studied the effects of cardiac denervation on free radical formation and infarct size in rats with reperfusion following prolonged ischemia and compared them with those of β-adrenoceptor blockade.

*(Received October 22, 2004; revised manuscript received January 27, 2005; accepted February 10, 2005)*

*The Second Department of Internal Medicine, *Department of Radiological Sciences, Toyama Medical and Pharmaceutical University, Toyama, Japan*

Mailing address: Takashi Nozawa, MD, The Second Department of Internal Medicine, Toyama Medical & Pharmaceutical University, 2630 Sugitani, Toyama 930-0194, Japan. E-mail: tnozawa@ms.toyama-mpu.ac.jp

## Methods

*Experimental Animal*

The experimental procedures were approved by the guidelines for animal experimentation at Toyama Medical and Pharmaceutical University. A total of 48 male Wistar rats weighing 300–350 g were used for induction of myocardial ischemia as described previously[14] Briefly, the rats were anesthetized with sodium pentobarbital (30 mg/kg, ip), and a left thoracotomy was performed to exteriorize the heart. The left coronary artery was ligated 2–3 mm from its origin with a suture of 5-0 prolene (Ethicon, Inc, Somerville, NJ, USA) for 30 min, and then the ligature was released.

The animals were divided into 3 groups: control, phenol, and atenolol. The following protocols were performed: (i) determination of hemodynamics and infarct size (control=8, phenol=6, atenolol=6), (ii) determination of interstitial NE concentrations during ischemia and reperfusion (control=7, phenol=4, atenolol=4), and (iii) electron paramagnetic resonance (EPR) study (control=6, phenol=7). One week before coronary ligation, regional cardiac denervation was performed by painting a solution of 10% phenol in ethanol on the left ventricular (LV) epicardium around the proximal region of the left coronary artery[15] The β1-selective adrenoceptor blockade, atenolol (0.5 mg/kg), was

**Table 1 Hemodynamic Data Before and During Coronary Artery Occlusion**

| | *Before* | | | *5 min after occlusion* | | | *20 min after occlusion* | | |
|---|---|---|---|---|---|---|---|---|---|
| | *Control (n=8)* | *Phenol (n=6)* | *Atenolol (n=6)* | *Control (n=8)* | *Phenol (n=6)* | *Atenolol (n=6)* | *Control (n=8)* | *Phenol (n=6)* | *Atenolol (n=6)* |
| *HR, beats/min* | 360±33 | 337±30 | 320±36 | 359±29 | 342±38 | 302±24* | 362±36 | 335±33 | 276±18**,† |
| *sBP, mmHg* | 104±22 | 119±21 | 108±15 | 109±30 | 104±8 | 85±11 | 112±27 | 108±9 | 83±14* |
| *dBP, mmHg* | 73±17 | 83±22 | 59±12 | 80±31 | 75±18 | 61±11 | 84±26 | 84±14 | 60±18 |
| *mBP, mmHg* | 84±18 | 96±20 | 68±10 | 92±29 | 86±15 | 71±13 | 96±24 | 93±10 | 69±15* |
| *RPP, $\times 10^2$ mmHg/min* | 372±80 | 397±58 | 346±62 | 396±129 | 355±30 | 255±41* | 410±124 | 362±41 | 228±47**,† |

*HR, heart rate; sBP, systolic blood pressure; dBP, diastolic BP; mBP, mean BP; RPP, rate pressure product; n, number of rats. Before indicates data obtained before coronary occlusion but after phenol painting or atenolol infusion. Data are means±SD. *p<0.05 and **p<0.01 vs control, †p<0.05 vs phenol.*

injected intravenously 10 min before the coronary ligation to block sympathetic effects![6]

In separate animals that underwent a sham operation without the coronary occlusion, cardiac NE concentrations were determined under conditions of normal innervation (n=5) and of sympathetic denervation with phenol painting (n=6). The NE concentration in the LV free wall was determined 1 week after the operation by high-performance liquid chromatography as described previously![7]

*Hemodynamic Study*

Cardiac hemodynamics were determined just before the coronary occlusion and at 5 and 20 min after inducing coronary occlusion. A 2F micromanometer-tipped catheter was inserted into the right carotid artery to measure aortic pressure. With the rat anesthetized and mechanically ventilated, aortic pressure and electrocardiogram were recorded, and digitized on-line at 2-ms intervals and analyzed with a signal-processing computer system (7T-18, NEC San-Ei, Tokyo, Japan).

*Myocardial Infarct Size*

The area at risk and infarct area were determined 2 h after reperfusion. Using the Langendorff technique, the hearts were isolated and perfused with Krebs solution at 37°C under perfusion pressure of 100 cm$H_2O$ for 5 min to remove the blood. Then 0.5 ml of blue ink was infused into the aorta after re-occlusion of the left coronary artery. Thereafter the LV was sliced into 2-mm thick sections for incubation in 1% triphenyl tetrazolium solution in phosphate buffer at 37°C for 10 min to distinguish stained viable tissue and unstained necrotic tissue. The area at risk and infarct area were determined using computerized planimetry.

*Interstitial NE Concentration*

Determination of the interstitial NE concentration during ischemia was performed using a microdialysis method. Rats were anesthetized with pentobarbital sodium (30 mg/kg, ip), followed by its continuous intravenous infusion (3 mg·$kg^{-1}\cdot h^{-1}$). Body temperature was maintained with a heated pad and lamp. The heart was exposed by midline incision and the microdialysis probe was inserted into the myocardium along the left coronary artery. Both ends of the dialysis fiber (8 mm length, 0.31 mm outer diameter, 0.2 mm inner diameter, and 50,000 molecular weight cutoff, PAN-130SF, Asahi Chemical, Japan) were connected to polyethylene tubes![8] The dialysis probe was perfused with Ringer's solution at a rate of 2 μl/min. Dialysate sampling before the coronary occlusion was started 60 min after probe implantation. Then the left coronary artery was ligated in the same method as described before. Dialysate sampling was performed during coronary occlusion and from the onset of reperfusion for 15 min. The NE concentration of the dialysate was measured by high-performance liquid chromatography with electrochemical detection (ECD 300, Eicom, Japan). After dialysate sampling, the position of the microdialysis probe was confirmed using an infusion of blue dye.

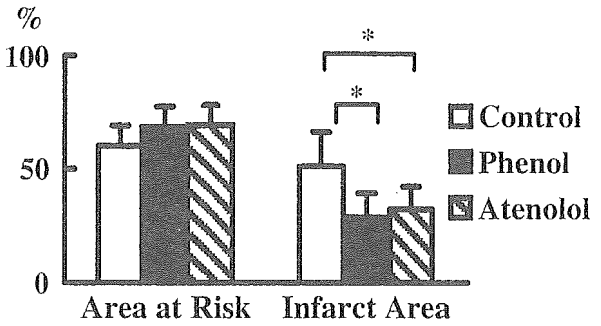


Fig 1. Area at risk (Left) and infarct area (Right) following 30-min of ischemia and 2-h of reperfusion. Risk area is presented as the percentage of the total left ventricular mass. Infarct size is presented as the percentage of the risk area. Area at risk was 60.0±9.5, 67.9±9.2, 69.3±9.5% and infarct area was 50.6±14.7, 28.5±11.3, 31.8±10.7% in the control, phenol, and atenolol group, respectively. Data are means+SD. *p<0.05.

*EPR Spin Trapping*

The spin trapping study was performed using 5,5-dimethyl-1-pyrroline-N-oxide (DMPO) as the spin trap. The microdialysis probe was perfused with Ringer's solution containing 1 mol/L DMPO at a rate of 6 μl/min. The dialysate was sampled 10 min before the coronary occlusion, 20 min after coronary occlusion, and 30, 60 and 120 min after reperfusion. Using 9.425-GHz field modulation with a 0.1-mT amplitude using microwave power of 4 mW, the EPR spectra of the microdialysate in a quartz-flat cell were recorded with EPR (RFR-30, Radical Research Inc, Tokyo, Japan) at room temperature. The yields of spin adducts were determined using a stable nitroxide radical, 4-hydroxy-2,2,6,6-tetramethyl-1-piperidineyloxy as the standard. A calibration curve was determined by plotting the product of peak-to-peak derivative amplitude and the square of the width at the maximum slope of the signal vs different concentrations of the standard nitroxide radical as described previously![9]

*Analysis of Data*

Data are expressed as mean±SD. Group comparisons were made using ANOVA followed by Bonferroni's t-test

Table 2 Interstitial Norepinephrine Concentration

| | Before | Coronary occlusion | | Reperfusion |
|---|---|---|---|---|
| | | 0–15 min | 15–30 min | 0–15 min |
| Control (pg/ml) (n=7) | 96±99 | 1,092±404 | 18,699±6,099 | 8,690±3,817 |
| Phenol (pg/ml) (n=4) | 17±20 | 9±12* | 6±9* | 28±26* |
| Atenolol (pg/ml) (n=4) | 15±10 | 3,054±1,531† | 23,826±9,640† | 5,875±1,441† |

Data are means±SD. *$p<0.01$ vs control, †$p<0.01$ vs phenol.

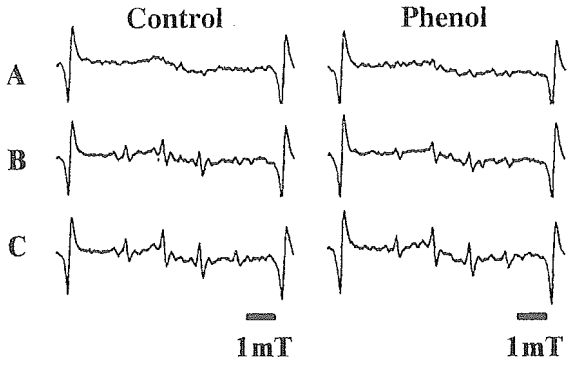


Fig 2. Representative EPR spectra of DMPO adducts in the microdialysate. (A) Signals before coronary occlusion. (B) Signals 30 min after reperfusion. (C) Signals 60 min after reperfusion. There was no significant difference between the control and phenol groups.

to identify differences between the various groups. A value of $p<0.05$ was considered statistically significant.

## Results

*Sympathetic Denervation by Phenol*

In the sham-operated rats, phenol depleted the tissue content of NE in the LV free wall (17±22 ng/g, n=6) compared with those without phenol (531±45 ng/g, n=5, $p<0.01$), a finding supporting complete sympathetic denervation by epicardial painting with phenol.

*Hemodynamics and Infarct Size*

The hemodynamic data during the 30-min coronary occlusion are shown in Table 1. Heart rate and blood pressure during the occlusion were lower in the atenolol group than in the control group, and consequently the rate–pressure product was smaller in the former. However, these indices did not differ significantly between the control and phenol groups, although they showed a trend toward a decrease in the phenol group. The size of the area at risk did not differ among the 3 groups; however, in the phenol group there was a significantly reduced ratio of infarct area to area at risk as compared with the control group (Fig 1). The ratio was also lower in the atenolol group than in the controls but did not differ between the phenol and atenolol groups.

*Interstitial Concentration of NE*

The interstitial NE concentration assessed by the microdialysis method tended to be lower in the phenol group than in the control group before the coronary occlusion, although the difference did not reach the significance level. During the coronary occlusion, its concentration increased markedly in the control group, but remained at quite low levels in the phenol group (Table 2). The NE concentration in the control group markedly decreased immediately after reperfusion but was still greater than in the phenol group. Atenolol did not affect the NE concentration during ischemia or reperfusion.

*Free Radical Formation in Ischemia–Reperfusion Injury*

Representative examples of EPR spectra are shown in Fig 2. There were no major components in the EPR spectra before the coronary occlusion, but 30 and 60 min after reperfusion, spectra consisting of a 1:2:2:1 quartet were observed. The equal nitrogen and hydrogen hyperfine coupling constants ($a_N = a^{\beta}_H = 1.49$ mT) in the spectra are characteristic of the hydroxyl radical adduct of DMPO (DMPO-OH).[20] Because the intensities of the EPR spectra are directly proportional to the free radical content in the microdialysate, a time course of spin-adduct generation can be compared with the control (Table 3). In the control group, no free radical generation was observed before ischemia, but a significant amount of spin adducts was detected after reperfusion and was maximal at 60 min after reperfusion was begun. Free radical formation in the phenol group was not significantly different from that of the control group.

## Discussion

The major findings of the present study are as follows. First, phenol painting of the epicardial surface at the proximal portion of the left coronary artery depleted the myocardial NE content as reported previously[15] and completely suppressed any increases in interstitial NE concentration during ischemia and subsequent reperfusion, a finding compatible with sympathetic denervation. Second, cardiac denervation significantly reduced the size of the infarct induced by ischemia–reperfusion injury and the reduction

Table 3 DMPO-OH EPR Signal Before and After Reperfusion

| | Before | Coronary occlusion | Reperfusion | | |
|---|---|---|---|---|---|
| | | 20–30 min | 30–40 min | 60–70 min | 120–130 min |
| Control (n=6) | ND | ND | 0.31±0.01 | 0.45±0.19 | 0.24±0.20 |
| Phenol (n=7) | ND | ND | 0.28±0.11 | 0.32±0.15 | NA |

ND, not detected. NA, not applicable. Data are means±SD. Ratios [the first peak of EPR signal from sample/signal from internal standard ($Mn^{2+}$)] are shown. One unit is calculated to be 1.58 μmol/L of nitroxide concentration.

was similar in the phenol and atenolol groups. Finally, the marked reduction of interstitial NE concentration caused by denervation was not accompanied by decreases in ·OH radical formation during reperfusion. Thus, NE-derived free radicals might not significantly contribute to the expansion of the infarct during ischemia–reperfusion injury.

*Effect of Denervation on Ischemic Injury*

Cardiac sympathetic innervation is suspected to exert a detrimental influence during ischemia. Previous studies[21–23] showed the beneficial effects of cardiac denervation on infarct size during ischemia. Other studies, however, demonstrated that cardiac denervation had no protective effect[24] or rather had a detrimental influence?[25] These conflicting findings may come from differences in the experimental methods (ie, pharmacological or surgical denervation, whole body or local cardiac denervation, isolated or in situ hearts, anesthetized or conscious animals, and the animal species used in each experiment). Another important issue that could result in conflicting data might be differences in the duration of coronary artery occlusion. A long period of ischemia may mask the beneficial effect of cardiac denervation. Elson et al demonstrated that cardiac denervation exerted a beneficial effect against myocardial necrosis by prolonging the time required for necrosis to develop after brief (40 min) coronary occlusion, but not when coronary occlusion was maintained for 80 min?[26]

Several mechanisms for the inhibition of ischemic injury in denervated hearts have been proposed. First, sympathetic denervation might induce the development of collateral vessels. Jones et al[22]) showed that coronary flow in the ischemic zone induced by ligation of the left anterior descending coronary artery was 2–4-fold greater in the chronically denervated dog heart than in the control heart. On the other hand, chronic, pharmacological denervation did not affect collateral flow during ischemia in rabbit hearts?[24] These disparate results might be related to species differences (ie, rabbit hearts have very few native collateral vessels compared with dog hearts). A poor native collateral network might respond poorly to myocardial ischemia in terms of collateral development after sympathectomy?[22,27] Rat hearts also have relatively poor native collateral network[28] and therefore the beneficial effects of denervation in the present study may not have resulted from increased collateral flow.

Second, adrenergic stimulation increases the oxygen requirement of the myocardium. During the 30-min coronary occlusion of the present study, the interstitial concentrations of NE increased more than 200-fold compared with before coronary occlusion in the control rats, but did not increase in the denervated rats. The number of $\beta$- and $\alpha_1$-adrenoceptors in the sarcolemmal membrane increases during myocardial ischemia without changes in the affinity to their agonists?[29] In fact, the activation of adenylyl cyclase activity was enhanced during the early period of ischemia?[30] Schömig clearly demonstrated that during 20–40 min of ischemia, the extracellular concentration of NE from nonexocytotic local metabolic release reaches 100–1,000-fold normal plasma concentration? Such a concentration of NE is capable of producing myocardial necrosis even in the nonischemic heart! Increases in cytosolic $Ca^{2+}$ induced by $\beta$- and $\alpha_1$-adrenoceptor stimulation would result not only in myofilament overstimulation, increased contractile force and oxygen requirement, but also excessive ATP breakdown. The increased cytosolic $Ca^{2+}$ can activate phospholipase that may cause membrane damage?[3,31,32]

These detrimental effects of NE would be inhibited by $\beta$-adrenoceptor blockade, as shown in previous studies[33,34] and the present study. In the present study the reduction in the size of the infarct by atenolol was comparable with that of denervation induced by phenol, despite a lower heart rate and smaller rate–pressure product in the atenolol group, indicating a lower oxygen requirement in that group. This finding suggests that cardiac denervation may have beneficial effects other than $\beta$-adrenoceptor blockade during ischemia or that the reduction in oxygen demand observed in the present study might not be sufficient to affect ischemic injury.

*Effects of Denervation on Reperfusion Injury*

Many mechanisms have been proposed to explain reperfusion injury, but the most plausible involve cytosolic calcium overload and the formation of oxygen-derived free radicals?[6–10] NE is a source of toxic free radicals during ischemia–reperfusion by amine oxidase and by auto-oxidation, and leads to the formation of cytotoxic ·OH radicals. Obata et al showed that sympathetic nerve stimulation generated cardiac interstitial ·OH radicals in association with increases in interstitial NE concentration![13] It is therefore likely that free radicals play an important role in catecholamine-induced cardiotoxicity by causing peroxidation of membrane phospholipids, which can result in permeability changes in the membrane, as well as intracellular calcium overload![11,35]

In the present study, the relationship between cardiac interstitial free radicals and infarct size was studied using cardiac microdialysis and EPR spin trapping in rats with normal cardiac innervation and with denervation. The intensities of the ·OH radicals were maximal at 60 min after reperfusion, a finding consistent with that of a previous study?[36] Despite a marked reduction of the interstitial NE concentration during ischemia and reperfusion in rats with denervation, the levels of ·OH radicals were not significantly different from those in rats with normal innervation, suggesting that NE might not be a major source of free radicals, at least under the present experimental conditions. There are a number of metabolic pathways whereby free radicals may be generated following reperfusion, but activated neutrophils, xanthine oxidase reaction, and mitochondrial respiration are the likely major sources?[6–10] The present results also suggest that NE-derived free radical formation does not significantly contribute to the development of myocardial necrosis after reperfusion injury.

There is considerable controversy as to whether free radicals cause myocyte death or endothelial injury. Several investigators reported infarct size limitation after the administration of superoxide dismutase with or without catalase?[37,38] but others have been unable to detect a protective effect with those treatments?[39–41] Those results may be related to differences in experimental methods, including the method of infarct size determination.

Reactive hyperemia early after reperfusion might contribute to the subsequent reperfusion injury. Reperfusion at reduced flow rates enhances postischemic contractile recovery?[42] Brunvand et al demonstrated that $\beta$-adrenoceptor blockade inhibited reperfusion hyperemia and reduced infarct size in feline hearts?[43] The reduction in the infarct by denervation in the present study may have been partially induced by suppression of reactive hyperemia, because NE release during ischemia and reperfusion was completely

inhibited. The inhibition of the $Na^+$–$H^+$ exchanger might be related to a reduced infarct size induced by cardiac denervation, because another study showed that it was activated during ischemia and its inhibition reduced infarct size during ischemia–reperfusion.[44]

*Study Limitations*

Some methodological limitations deserve comment in interpreting the present results. First, we only detected DMPO-OH adducts showing an EPR spectrum consisting of a 1:2:2:1 quartet in the EPR spin trapping study. Relatively unstable free radical adducts of DMPO such as the $O_2^{\cdot-}$ adduct of DMPO (DMPO-OOH, half time about 60 s at pH 7.0)[45] might not be detected by our methods, which required 10 min to collect interstitial fluid for EPR spin trapping. In the very early phase of reperfusion, there is an initial prominent generation of oxyradicals, mainly $O_2^{\cdot-}$ radicals.[36] There are many sources of ·OH including the conversion from $O_2^{\cdot-}$, and the activation of lipid peroxidation and arachidonate metabolism in a chain reaction. The $O_2^{\cdot-}$-adduct of DMPO is known to break down to form the DMPO-OH adduct[46] and, therefore, some of the observed DMPO-OH signal could be caused by trapping of $O_2^{\cdot-}$. A previous study reported the generation of superoxide during ischemia,[37] but the EPR spectra of DMPO adducts were not detected during coronary occlusion before reperfusion in the present study. Further work using radical scavengers is needed to elucidate the source of ·OH and their effects on myocardial reperfusion injury.

Second, hemodynamic differences among the 3 groups might contribute to the differences in infarct size. The rate–pressure product during the coronary occlusion was lower in the atenolol group than in the other 2 groups and, therefore, a greater decrease in oxygen demand in the rats with atenolol might partially contribute to the reduction in infarct size. An equivalent reduction of infarct size between the phenol and atenolol groups despite their hemodynamic differences suggests more complete inhibition of the influence of NE in the phenol group or the contribution of some factors other than inhibition of $\beta$-adrenoceptors (eg, $\alpha$-adrenoceptors could be involved in the reduction of infarct size in the phenol group).

## Conclusion

We studied the effects of cardiac denervation on in vivo ischemia–reperfusion injury in terms of cardiac interstitial NE concentration and oxygen free radicals. The concentrations of interstitial NE increased more than 200-fold during 30-min ischemia in normally innervated hearts and the complete inhibition of increasing interstitial NE by denervation significantly reduced the size of the infarct caused by ischemia–reperfusion injury. Although the mechanism of the infarct-limiting effect of cardiac denervation remains unclear, it more likely results primarily from decreasing the direct activation of $\beta$-adrenergic signaling, not from decreasing NE-derived free radicals.

## References


1. Waldenström AP, Hjalmarson AC, Tornell L. A possible role of noradrenaline in the development of myocardial infarction. *Am Heart J* 1978; **95:** 43–51.
2. Hara A, Abiko Y. Role of the sympathetic nervous system in the ischemic and re-perfused heart. *EXS* 1996; **76:** 285–297.
3. Rona G. Cathecholamine cardiotoxicity. *J Mol Cell Cardiol* 1985; **17:** 291–306.
4. Kawabata M, Kubo I, Suzuki K, Terai T, Iwama T, Isobe M. 'Tako-Tsubo cardiomyopathy' associated with syndrome malin: Reversible left ventricular dysfunction. *Circ J* 2003; **67:** 745–749.
5. Schömig A. Catecholamines in myocardial ischemia: Systemic and cardiac release. *Circulation* 1990; **82**(Suppl II): II-13–II-22.
6. Ambrosio G, Tritto I. Reperfusion injury: Experimental evidence and clinical implications. *Am Heart J* 1999; **138:** S69–S75.
7. Park JL, Lucchesi BR. Mechanisms of myocardial reperfusion injury. *Ann Thorac Surg* 1999; **68:** 1905–1912.
8. Williams FM. Neutrophils and myocardial reperfusion injury. *Pharmacol Ther* 1996; **72:** 1–12.
9. Lucchesi BR. Myocardial ischemia, reperfusion and free radical injury. *Am J Cardiol* 1990; **65:** 14I–23I.
10. Kinugasa Y, Ogino K, Furuse Y, Shiomi T, Tsutsui H, Yamamoto T, et al. Allopurinol improves cardiac dysfunction after ischemia-reperfusion via reduction of oxidative stress in isolated perfused rat hearts. *Circ J* 2003; **67:** 781–787.
11. Singal PK, Kapur N, Dhillon KS, Beamish RE, Dhalla NS. Role of free radicals in catecholamine-induced cardiomyopathy. *Can J Physiol Pharmacol* 1981; **60:** 1390–1397.
12. Obata T, Hosokawa H, Yamanaka Y. In vivo monitoring of norepinephrine and ·OH generation on myocardial ischemic injury by dialysis technique. *Am J Physiol* 1994; **35:** H903–H908.
13. Obata T, Yamanaka Y. Cardiac microdialysis of salicylic acid ·OH generation on nonenzymatic oxidation by norepinephrine in rat heart. *Biochem Pharmacol* 1997; **53:** 1375–1378.
14. Igawa A, Nozawa T, Yoshida N, Fujii N, Inoue M, Tazawa S, et al. Heterogeneous cardiac sympathetic innervation in heart failure after myocardial infarction of rats. *Am J Physiol* 2000; **278:** H1134–H1141.
15. Mori H, Pisarri TE, Aldea GS, Husseini WK, Dae MW, Stevens MB, et al. Usefulness and limitations of regional cardiac sympathectomy by phenol. *Am J Physiol* 1989; **257:** H1523–H1533.
16. Desprès G, Veissier I, Boissy A. Effect of autonomic blockers on heart period variability in calves: Evaluation of the sympatho-vagal balance. *Physiol Res* 2002; **51:** 347–353.
17. Nozawa T, Igawa A, Yoshida N, Maeda M, Inoue M, Yamamura Y, et al. Dual-tracer assessment of coupling between cardiac sympathetic neuronal function and downregulation of $\beta$-receptors during development of hypertensive heart failure of rats. *Circulation* 1998; **97:** 2359–2367.
18. Yamazaki T, Akiyama T, Shindo T. Routine high-performance liquid chromatographic determination of myocardial interstitial norepinephrine. *J Chromatogr B Biomed Appl* 1995; **670:** 328–331.
19. Honda H, Zhao Q, Kondo T. Effects of dissolved gases and an echo contrast agent on apoptosis induced by ultrasound and its mechanism via the mitochondria-caspase pathway. *Ultrasound Med Biol* 2002; **28:** 673–682.
20. Buettner GR. Spin trapping: ESR parameters of spin adducts. *Free Radic Biol Med* 1987; **3:** 259–303.
21. Jones CE, Devous MD Sr, Thomas JX Jr, DuPont E. The effect of chronic cardiac denervation on infarct size following acute coronary occlusion. *Am Heart J* 1978; **95:** 738–746.
22. Jones CE, Beck LY, DuPont E, Barnes GE. Effects of coronary ligation of the chronically sympathectomized dog ventricle. *Am J Physiol* 1978; **235:** H429–H434.
23. Barber MJ, Thomas JX Jr, Jones SB, Randall WC. Effect of sympathetic nerve stimulation and cardiac denervation on MBF during LAD occlusion. *Am J Physiol* 1982; **243:** H566–H574.
24. Matsuki T, Cohen MV, Holt G, Ayling J, Hearse DJ, Downey JM. Chronic whole body sympathectomy fails to protect ischemic rabbit heart. *Am J Physiol* 1989; **256:** H1322–H1327.
25. Lavallee M, Amano J, Vatner SF, Manders WT, Randall WC, Thomas JX Jr. Adverse effects of chronic cardiac denervation in conscious dogs with myocardial ischemia. *Circ Res* 1985; **57:** 383–392.
26. Elson JJ, Ten Eick RE, Singer DH. Autonomic nervous system and cellular injury from circumflex ligation in dogs. *Am J Physiol* 1981; **240:** H738–H745.
27. Jones CE, Scheel KW. Reduced coronary collateral resistance after chronic ventricular sympathectomy. *Am J Physiol* 1980; **238:** H196–H201.
28. Maxwell MP, Hearse DJ, Yellon DM. Species variation in the coronary collateral circulation during regional myocardial ischaemia: A critical determinant of the rate of evolution and extent of myocardial infarction. *Cardiovasc Res* 1987; **21:** 737–746.
29. Maisel AS, Motulsky HJ, Ziegler MG, Insel PA. Ischemia- and agonist-induced changes in $\alpha$- and $\beta$-adrenergic receptor traffic in guinea pig hearts. *Am J Physiol* 1987; **253:** H1159–H1166.
30. Strasser RH, Krimmer J, Braun-Dullaeus R, Marquetant R, Kübler

W. Dual sensitization of the adrenergic system in early myocardial ischemia: Independent regulation of the β-adrenergic receptors and the adenylyl cyclase. *J Mol Cell Cardiol* 1990; **22:** 1405–1423.
31. Gotzsche O. Decreased myocardial calcium uptake after isoproterenol in streptozotocin-induced diabetic rats. *Lab Invest* 1983; **48:** 156–161.
32. Lubbe WH, Podzuweit T, Opie LH. Potential arrythmogenic role of cyclic adenosine monophosphate (AMP) and cytosolic calcium overload: Implications for prophylactic effects of beta-blockers in myocardial infarction and proarrythmic effects of phosphodiesterase inhibitors. *J Am Coll Cardiol* 1992; **19:** 1622–1633.
33. Bril A, Slivjak M, DiMartino MJ, Feuerstein GZ, Linee P, Poyser RH, et al. Cardioprotective effects of carvedilol, a novel β-adrenoceptor antagonist with vasodilating properties, in anaesthetized minipigs: Comparison with propranolol. *Cardiovasc Res* 1992; **26:** 518–525.
34. Burmeister WE, Reynolds RD, Lee RJ. Limitation of myocardial infarct size by atenolol, nadolol and propranolol in dogs. *Eur J Pharmacol* 1981; **75:** 7–10.
35. Josephson RA, Silverman HS, Lakatta EG, Stern MD, Zweier JL. Study of the mechanism of hydrogen peroxide and hydroxyl free radical-induced cellular injury and calcium overload in cardiac myocytes. *J Biol Chem* 1991; **266:** 2354–2361.
36. Kuzuya T, Hoshida S, Kim Y, Nishida M, Fuji H, Kitabatake A, et al. Detection of oxygen-derived free radical generation in the canine postischemic heart during late phase of reperfusion. *Circ Res* 1990; **66:** 1160–1165.
37. Jolly SR, Kane WJ, Bailie MB, Abrams GD, Lucchhesi BR. Canine myocardial reperfusion injury: Its reduction by the combined administration of superoxide dismutase and catalase. *Circ Res* 1984; **54:** 277–285.
38. Ambrosio G, Becker LC, Hutchins GM, Weisman HF, Weisfeldt ML. Reduction in experimental infarct size by recombinant human superoxide dismutase: Insights into the pathophysiology of reperfusion injury. *Circulation* 1986; **74:** 1424–1433.
39. Becker LB, Vanden Hoek TL, Shao Z, Li C, Shumacker PT. Generation of superoxide in cardiomyocytes during ischemia before reperfusion. *Am J Physiol* 1999; **277:** H2240–H2246.
40. Miki T, Choen MV, Downey JM. Failure of N-2-mercaptopropionyl glycine to reduce myocardial infarction after 3 days of reperfusion in rabbits. *Basic Res Cardiol* 1999; **94:** 180–187.
41. Richard VJ, Murry CE, Jennings RB, Reimer KA. Therapy to reduce free radicals during early reperfusion does not limit the size of myocardial infarcts caused by 90 min of ischemia in dogs. *Circulation* 1988; **78:** 473–480.
42. Takeo S, Liu JX, Tanonaka K, Nasa Y, Yabe K, Tanahashi H, et al. Reperfusion at reduced flow rates enhances postischemic contractile recovery of perfused heart. *Am J Physiol* 1995; **268:** H2384–H2395.
43. Brunvand H, Kvitting PM, Rynning SE, Berge RK, Grong K. Carvedilol protects against lethal reperfusion injury through antiadrenergic mechanisms. *J Cardiovasc Pharmacol* 1996; **28:** 409–417.
44. Karmazyn M, Gan XT, Humphreys RA, Yoshida H, Kusumoto K. The myocardial $Na^+$–$H^+$ exchange structure, regulation, and its role in heart disease. *Circ Res* 1999; **85:** 777–786.
45. Buettner GR, Oberley LW. Considerations in the spin trapping of superoxide and hydroxyl radical in aqueous systems using 5,5-dimethyl-1-pyrroline-1-oxide. *Biochem Biophys Res Commun* 1978; **83:** 69–74.
46. Finkelstein E, Rosen GM, Rauckman EJ. Spin trapping of superoxide and hydroxyl radical: Practical aspects. *Arch Biochem Biophys* 1980; **200:** 1–16.